Satellite Observations of a Severe Supercell Thunderstorm on 24 July 2000 Made during the *GOES-11* Science Test

JOHN F. WEAVER, JOHN A. KNAFF, AND DAN BIKOS

Regional and Mesoscale Meteorology Team, Cooperative Institute for Research in the Atmosphere, Fort Collins, Colorado

GARY S. WADE

NOAA/NESDIS/ORA/ARAD, Advanced Satellite Products Team, Madison, Wisconsin

JAIME M. DANIELS

NOAA/NESDIS/ORA/ARAD, Forecast Products Development Team, Camp Springs, Maryland

(Manuscript received 6 April 2001, in final form 20 August 2001)

ABSTRACT

This paper utilizes a severe thunderstorm case from 24 July 2000 to demonstrate the relevance of Geostationary Operational Environmental Satellite (GOES) rapid-scan imagery and sounder data in the short-range forecasting and nowcasting time frames. Results show how these data can be employed quickly and effectively during the warning decision-making process. Various aspects of the severe storm environment are identified that could only be diagnosed in this case using satellite data.

The data used in this study are unique in that the imager and sounder input both come from one of the newest of the geostationary satellites, *GOES-11*. The datasets were collected as a part of the satellite's 6-week science test. During this test period, continuous 1-min imagery and 30-min sounder data were available. The new satellite has now been placed on standby and will be put in service when either *GOES-East* or *GOES-West* fails.

Two new high-resolution satellite products are presented that are currently in the developmental phase. These will be field tested and implemented within the next couple of years.

1. Introduction

On 27 April 1994, the first of the National Oceanic and Atmospheric Administration's (NOAA) current series of Geostationary Operational Environmental Satellites, *GOES-8*, was launched. After an initial system testing period—known as the *GOES-8* science test—the satellite was placed in equatorial orbit at approximately 75°W where it is currently performing routine operations. Since then, three other satellites in this series have been launched: *GOES-9* (launched 23 May 1995; status, now on standby with mechanical difficulties), *GOES-10* (launched 25 April 1997; status, conducting routine operations at 135°W), and *GOES-11* (launched 3 May 2000; status, currently on standby in orbit, following its 6-week science test).[1] All of the current geostationary satellites are fitted with instruments that provide frequent scans of the Western Hemisphere in 5 imager and 19 sounder channels (18 thermal infrared, and 1 visible).

The science test period for *GOES-11* ran from 30 June to 13 August 2000. The first half of the 6-week period was devoted to testing system components and optimizing instrument performance; the latter half focused on capturing real-time weather events. During the second half of the experiment, the default scanning schedule called for the imager to routinely collect 5-min-interval imagery over the continental United States (CONUS), and the sounder to collect 30-min-interval data over a portion of the CONUS. Science test coordinators also had the option of increasing the scan frequency of the imager to a 1-min interval over a limited area to capture significant mesoscale weather events. This scheduling strategy is commonly referred to as super-rapid-scan operations, or SRSO. They could also increase the sounder scan interval to 10 min, but both rapid interval sounder data and SRSO imagery could not be collected simultaneously.

On 24 July 2000, NOAA's Storm Prediction Center issued a moderate risk for severe thunderstorms over

[1] Since this article was written, another satellite in the GOES series, *GOES-12*, was launched, underwent testing, and is also on standby, awaiting service.

Corresponding author address: John F. Weaver, NOAA/NESDIS/RAMM, CIRA Bldg., Foothills Campus, Colorado State University, Fort Collins, CO 80523.
E-mail: weaver@cira.colostate.edu

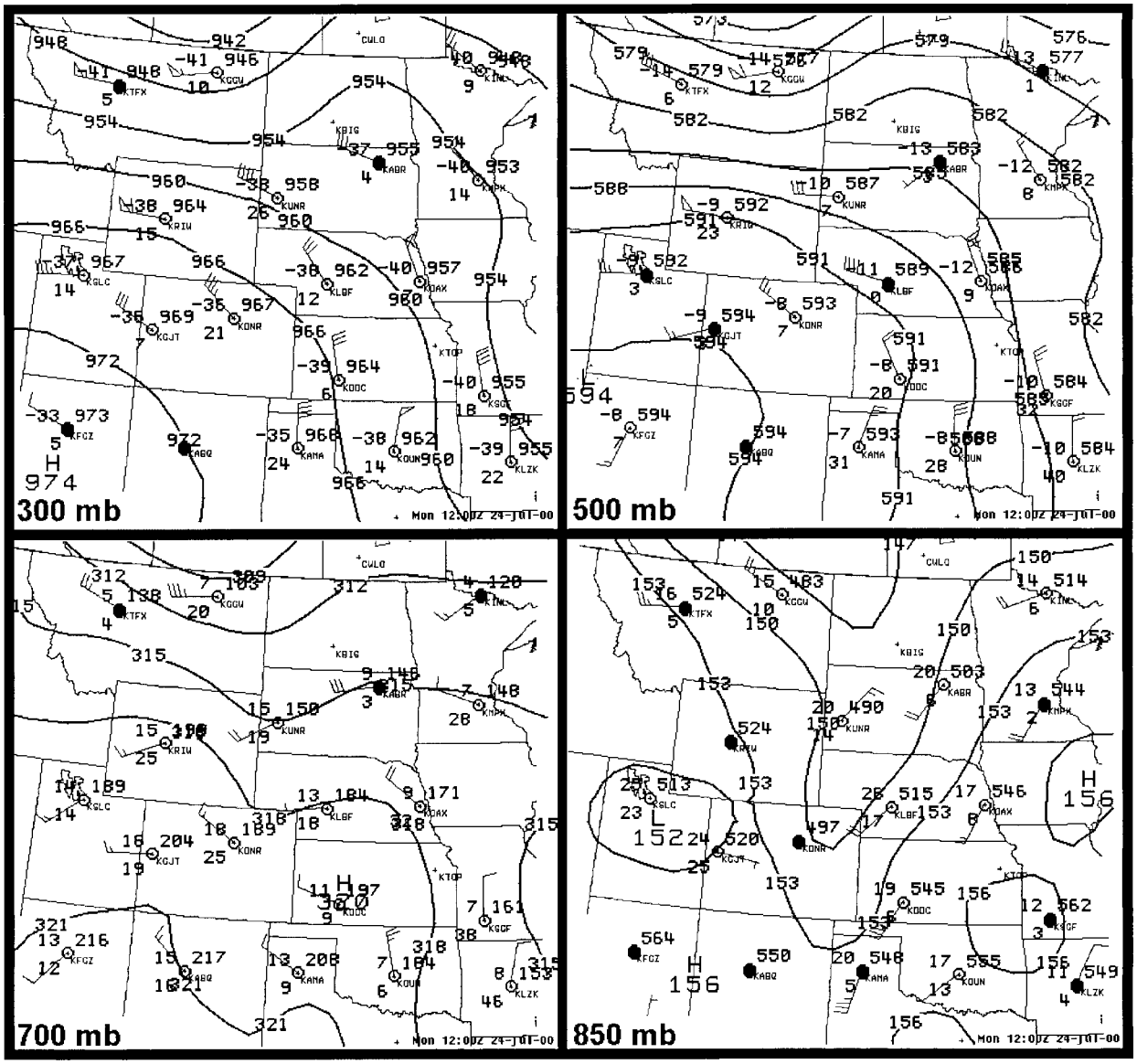

FIG. 1. NCEP-produced, synoptic height analyses from 1200 UTC on 24 Jul 2000. Station plots are U.S. standard. Heights are objectively analyzed. The four panels include analyses at 300, 500, 700, and 850 mb.

the central plains of the United States, and *GOES-11* project forecasters requested that the satellite be placed in its SRSO scan mode. The sector was centered at 44°N and 98°W. SRSO began at 1915 UTC and, at approximately 2130 UTC, a storm formed in south-central South Dakota at the intersection of an east–west-oriented mesoscale outflow boundary with a north–south-oriented trough. Shortly after forming, the storm appeared to split. The right-mover of the pair ended up traveling due south across central Nebraska. During a 10-h period, this supercell thunderstorm produced several incidents of hail exceeding 5 cm in diameter, and three confirmed tornado sightings—all of which were in rural areas.

This manuscript presents an overview of the synoptic environment, a description of the subsynoptic environment as it evolved throughout the day, and a review of the mesoscale aspects of storm morphology using both satellite imagery and radar data that were available during this event. The utility of rapid-scan imaging is discussed, and half-hourly products derived from the *GOES-11* sounder are presented that illustrate the added value of having routine, frequent interval sounder data available to forecasters.

2. Satellite datasets

The five standard channels on the current GOES series imagers include a visible channel (responding from 0.52 to 0.72 μm), as well as four infrared channels with

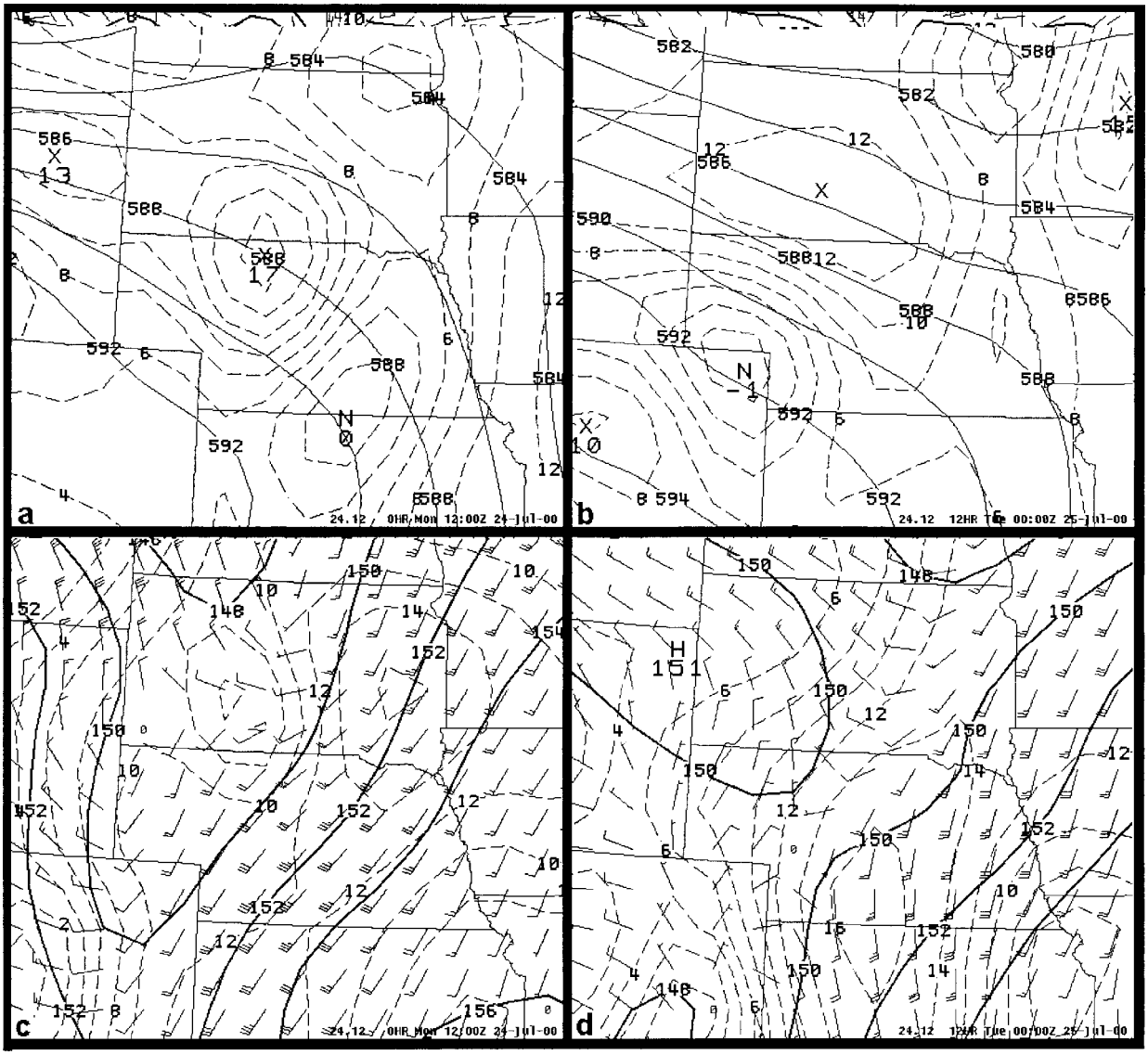

FIG. 2. Eta Model output for (a) initial analysis of 500-mb heights and vorticity valid at 1200 UTC 24 Jul 2000, (b) 12-h forecast of 500-mb heights and vorticity valid at 0000 UTC 25 Jul 2000, (c) initial analysis of 850-mb heights and dewpoints with wind barbs superimposed valid at 1200 UTC on 24 Jul 2000, and (d) 12-h forecast of 850-mb heights, dewpoints, and winds valid at 0000 UTC on 25 Jul 2000.

central wavelengths at 3.9 μm (used primarily to discriminate water from ice clouds), 6.7 μm (a channel sensitive to mid- and upper-level water vapor), 10.7 μm (a relatively uncontaminated window channel), and 12.0 μm (a window channel with a slight response to low-level water vapor).

The GOES sounder has instrumentation to measure emitted radiation in one visible wavelength band as well as in 18 thermal infrared bands that are primarily sensitive to carbon dioxide, water vapor, or ozone. From the responses to these variables at various wavelengths, atmospheric soundings can be constructed. The horizontal sampling resolution at satellite subpoint is approximately 8.7 km, with 13-bit data transmitted to GOES receiving facilities. For more information on the characteristics and capabilities of both the imager and sounder channels, refer to Menzel and Purdom (1994).

The full-time availability of the GOES sounder data allows for the generation of operational sounding products. A nonlinear physical retrieval algorithm (Ma et al. 1999) is applied to clear-sky sounder radiances in order to solve for surface skin temperature as well as profiles of temperature and moisture. First-guess temperature and moisture profiles for the retrieval algorithm are provided by a time–space interpolation of short-term (less than 12 h) Eta Model forecasts obtained from the National Centers for Environmental Prediction (NCEP). A radiance tuning process (Schmit 1996) is performed in order to remove bias differences between observed and calculated radiances. Hourly surface temperature and

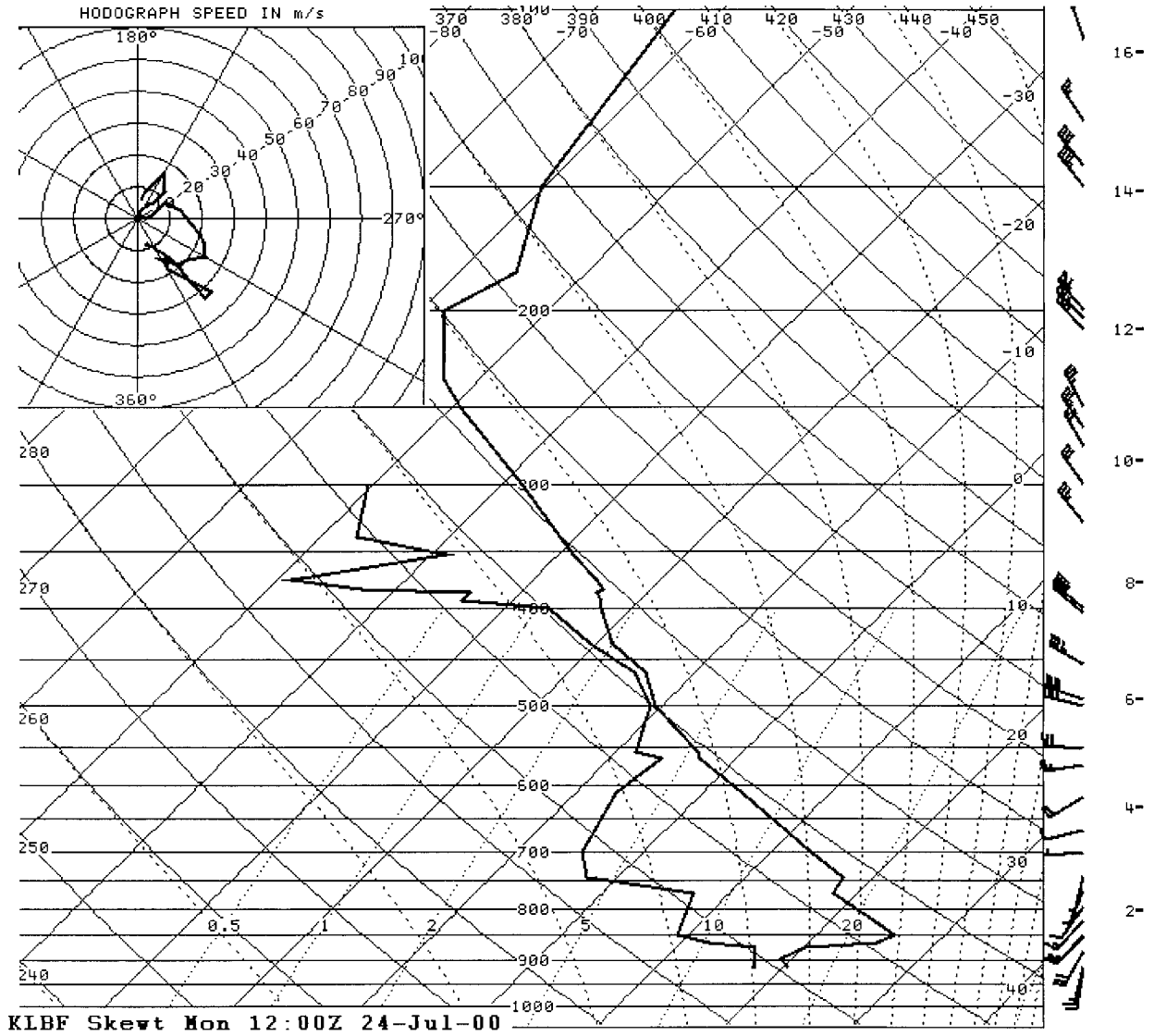

FIG. 3. Plot of radiosonde data from North Platte, NE (LBF), taken at 1200 UTC 24 Jul 2000. Plot shows temperature, dewpoint, and winds (in kt). Hodograph in upper-left corner.

moisture information are obtained from the National Weather Service's (NWS) Family of Services data network and analyzed for use as boundary conditions for the retrieval algorithm. The retrieved temperature and moisture profiles are then used to compute the various atmospheric stability indices described and shown in sections 3–5 of this paper. In the present study, horizontal fields of atmospheric stability and moisture parameters—with derived products such as convective available potential energy (CAPE), convective inhibition (CIN), and lifted index (LI)—are utilized.

Two versions of the sounder products will be presented. The first is produced at the Cooperative Institute for Meteorological Satellite Studies (CIMSS[2]) in Madison, Wisconsin, and displays results at a relatively coarse resolution (Hayden et al. 1996; Menzel et al. 1998). As noted, the detectors on the sounder instrument have a resolution of approximately 8.7 km on a side at subsatellite point. However, sampling (at subpoint) is performed only once every 10 km. This is why the sounder is said to have a ''nominal resolution'' of 10 km. Also, because the earth ''curves away'' from the satellite, the sensed-area becomes larger as the sample is taken at higher local zenith angles. For example, if the eastern sounder is taking samples over South Dakota, the resolution is roughly 12 km east–west by 16 km north–south. To reduce the signal-to-noise ratio, the final sounder images—known as derived product imagery (DPI)—at CIMSS are spatially averaged over a 3×3 field-of-view (FOV) box, which equates to an approximate DPI pixel size of a 36 km $\times$ 48 km area

[2] Real-time DPI from CIMSS can be accessed online at http://cimss.ssec.wisc.edu/goes/realtime/realtime.html.

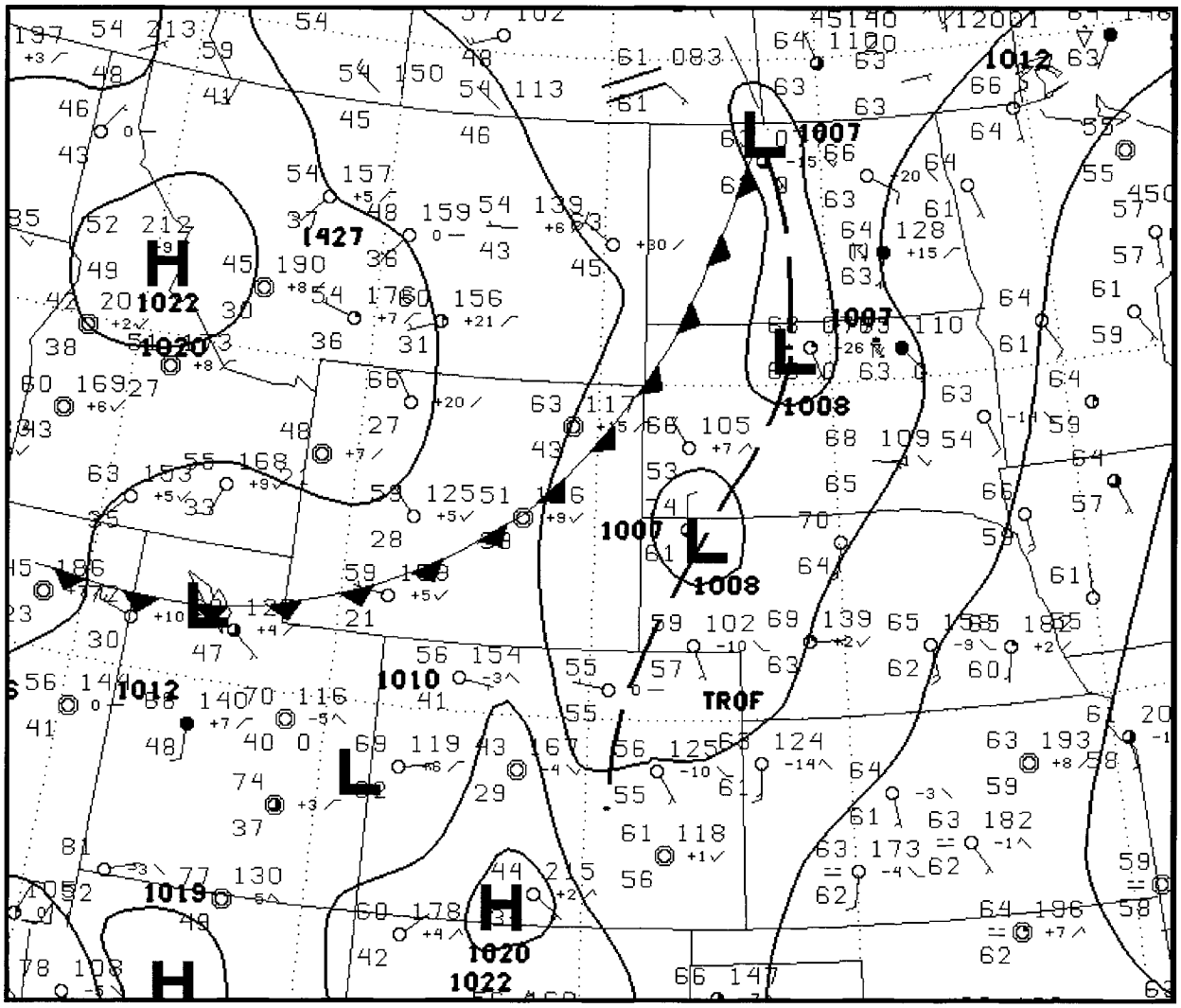

FIG. 4. NCEP surface pressure analysis over the north-central plains based on observations taken around 1200 UTC 24 Jul 2000. Plotting conventions and symbols are from standard U.S. charts.

over South Dakota. Cloudy areas are replaced by pixels from the 10.7-μm window data in the DPI imagery.

The second version of the sounder product presented in this paper is produced experimentally by National Environmental Satellite, Data, and Information Service (NESDIS), where the data are generated and displayed at full resolution. In the following discussion, this version will be referred to as the single field-of-view (SFOV) product. The retrieval algorithm used is the same as the one used in the CIMSS-retrieved product. The difference lies in the fact that the algorithm is applied to clear-sky sounder radiances at each measurement point as opposed to average sounder radiances computed from clear-sky radiance measurements made over the 3 $\times$ 3 FOV scene.

3. 24 July 2000 synoptic overview

Synoptic data from 1200 UTC on the morning of 24 July 2000 found the north-central Plains under northwesterly flow at mid- and upper levels (Fig. 1). A shortwave trough over South Dakota and Nebraska was exiting the region; a second was expected to arrive in the area by midafternoon (Figs. 1, 2a, and 2b). This second

→

FIG. 5. (a) *GOES-11* 10.7-μm image taken at 1650 UTC 24 Jul 2000. Image shows MCC exiting eastern SD and weaker convection in eastern NE, and (b) *GOES-11* visible wavelength satellite image taken at 2130 UTC 24 Jul 2000 over the same area as in (a). Image shows partly cloudy areas in eastern NE and an outflow boundary in southeast SD. White arrows indicate outflow boundary; black, the MCS remnants.

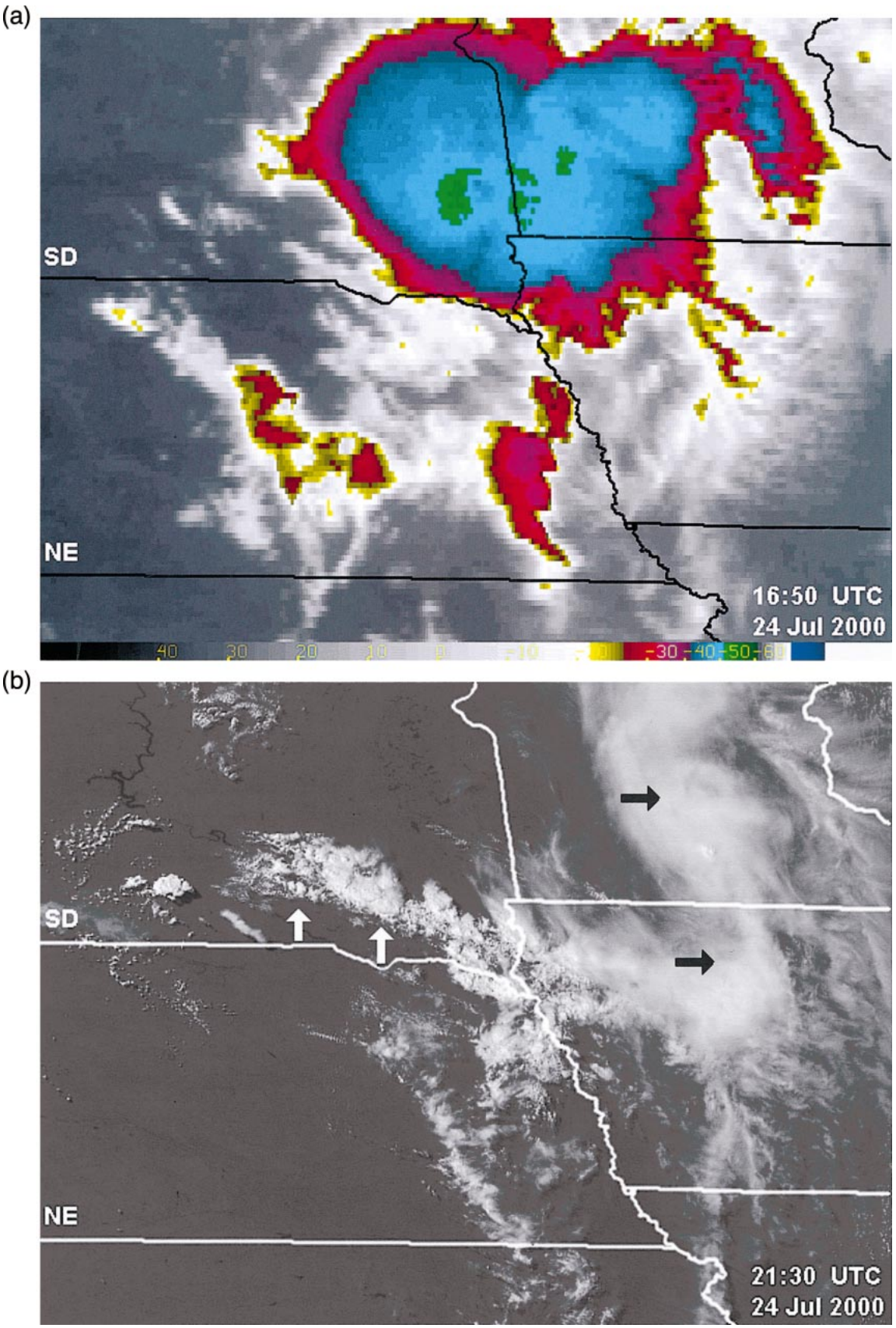
(a)
SD
NE
16:50 UTC
24 Jul 2000
40
30
20
10
0
-10
-30
-40
-50
-60
(b)
SD
NE
21:30 UTC
24 Jul 2000

(a)

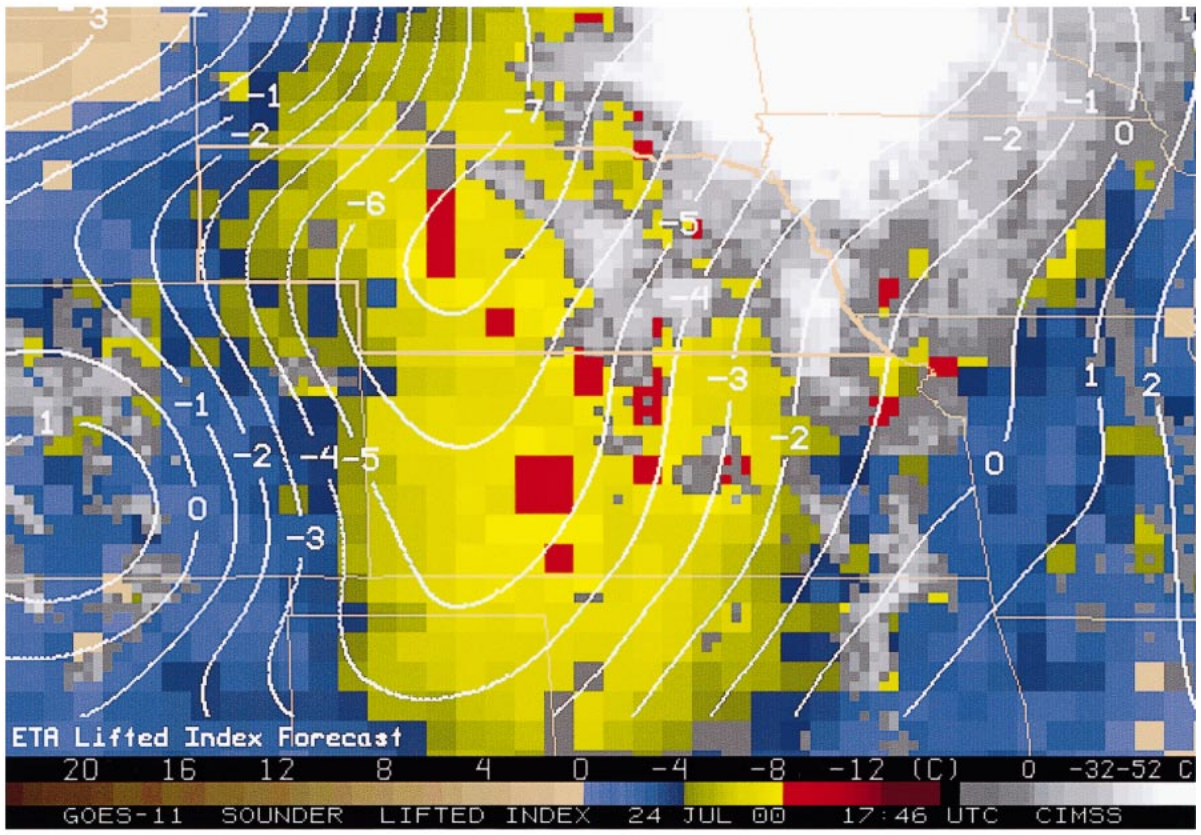
ETA Lifted Index Forecast
20 16 12 8 4 0 -4 -8 -12 (C) 0 -32-52 C
GOES-11 SOUNDER LIFTED INDEX 24 JUL 00 17:46 UTC CIMSS

(b)

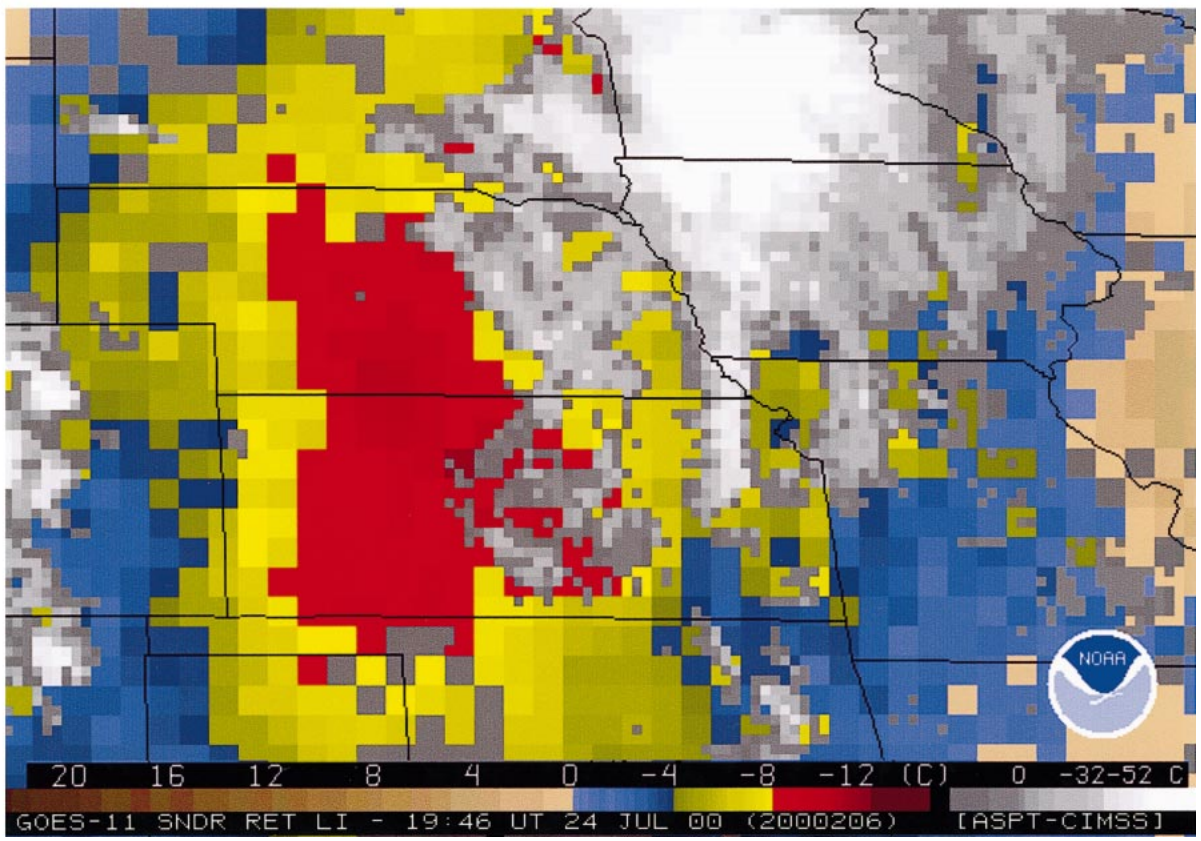
NOAA
20 16 12 8 4 0 -4 -8 -12 (C) 0 -32-52 C
GOES-11 SNDR RET LI - 19:46 UT 24 JUL 00 (2000206) [ASPT-CIMSS]

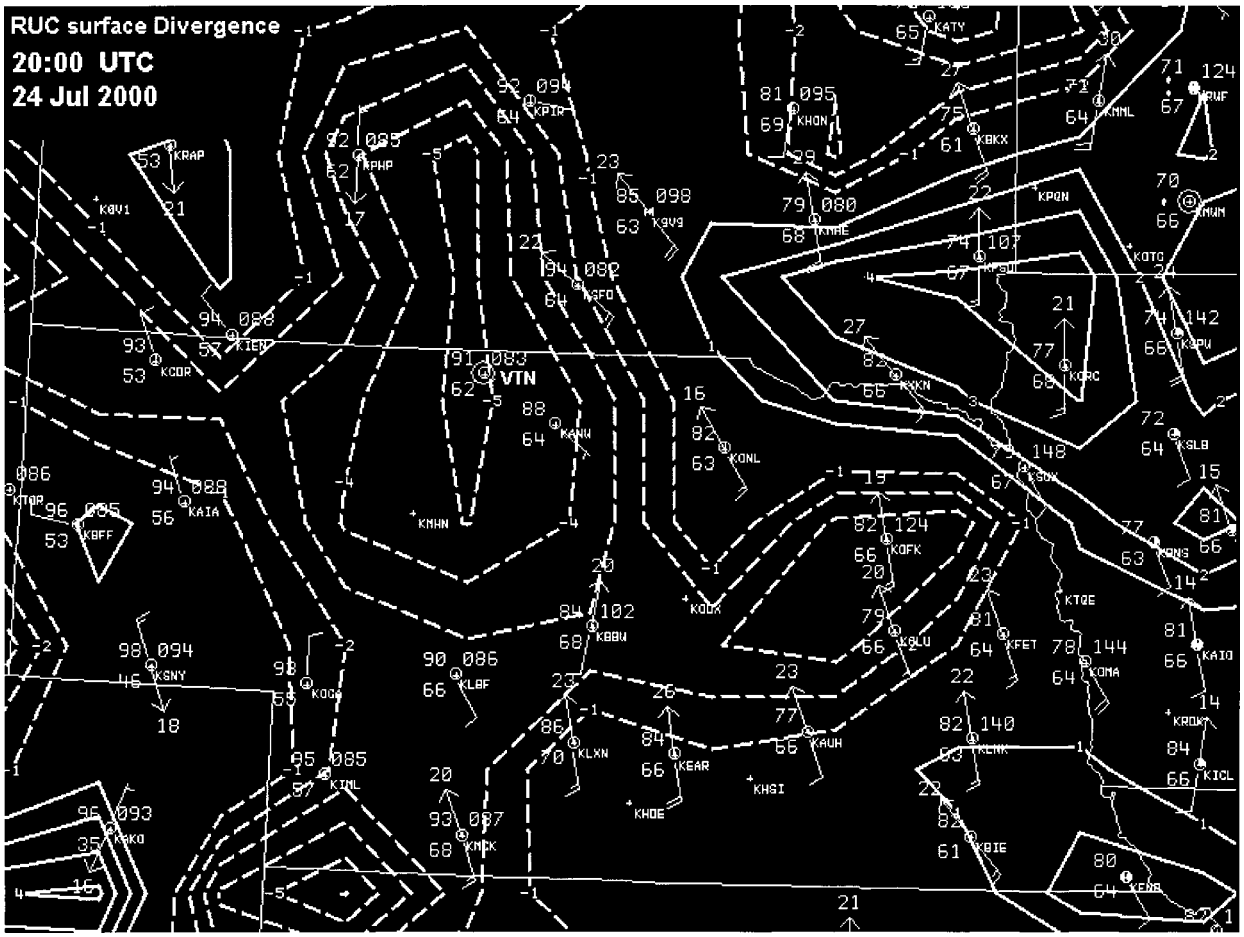

FIG. 7. Rapid Update Cycle (RUC) analysis of surface divergence superimposed on a map of standard surface observations. Observations and analysis both at 2000 UTC 24 Jul 2000.

disturbance was expected to provide support for the development of deep convection. Any storms that did develop were expected to become severe. Lapse rates in the area were nearly dry adiabatic in the lowest 5 km (Fig. 3). The CAPE, using a forecast mixed dewpoint value of 17°C (63°F) with the morning sounding at North Platte, was estimated at over 4000 J Kg^{-1}. This dewpoint estimate was realistic, given the anticipated low-level moisture advection into central Nebraska and south-central South Dakota (Figs. 2c, 2d). Last, the surface synoptic analysis revealed a surface low pressure area at the southern end of a broad trough in western Nebraska at 1200 UTC (Fig. 4). This feature was forecast to move into central Nebraska by late afternoon, bringing with it a trough to its south and backing winds in central and eastern sections of both South Dakota and Nebraska. The backing and intensifying winds would increase the marginally favorable shear [the 0–3-km storm relative environmental helicity (SREH) from the morning sounding was 122 $m^2\ s^{-2}$].

Based on the antecedent conditions, NOAA's Storm Prediction Center issued an outlook for a moderate risk of severe thunderstorms over the central plains of the United States, and *GOES-11* science-test forecasters requested that the new satellite's imager be placed in its SRSO mode beginning at 1915 UTC. The idea was to anticipate convective development by at least 90 min. The request specified that the sector be centered over the South Dakota–Nebraska region. Forecasters also asked that SRSO continue over a 24-h period, since the unstable air mass was expected to remain in place throughout the night.

←

FIG. 6. Surface-based lifted index image computed from *GOES-11* sounder data (a) overlaid with the Eta Model 6-h forecast LI field for beginning image scan time of 1746 UTC. Model forecast valid time is 1800 UTC. Central column of states (from top to bottom) are SD, NE, KS, and OK and (b) same as in (a) except time is 1946 UTC and Eta Model overlay not available.

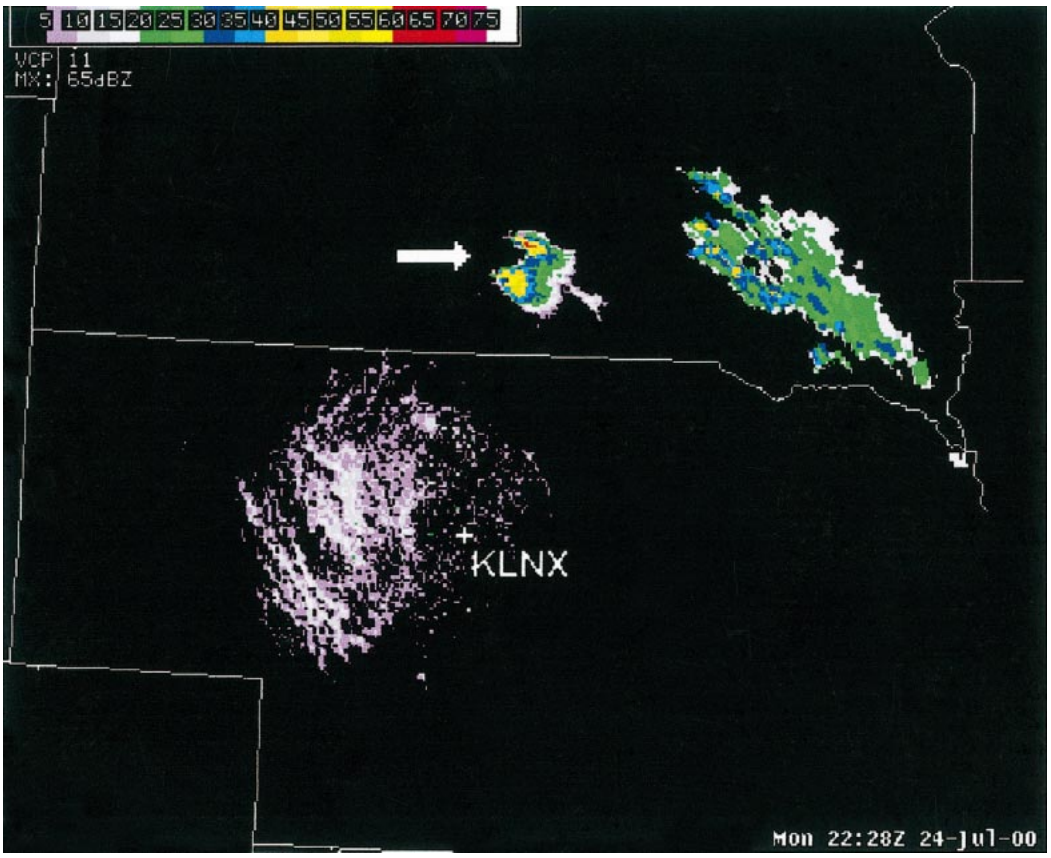

FIG. 8. The 0.5° tilt, PPI radar reflectivity data from the WSR-88D located at Thedford, NE (KLNX). Scan start time is 2228 UTC 24 Jul 2000. Arrow points to splitting cell in southern SD.

4. Modifications to the model forecast output with subsynoptic data

The morning Eta Model run suggested that CAPE values in excess of 2400 J Kg^{-1} (corresponding minimum surface-based lifted indices were -7) would develop by noon in the area of interest. This estimate seems reasonable, given the analysis of the North Platte, Nebraska (LBF) sounding that suggested a CAPE value of over 4000 J Kg^{-1} by late afternoon. The Eta Model output also indicated that a narrow axis of maximum instability, stretching from extreme southwest Nebraska into northeastern South Dakota (and beyond), would develop. As will be shown, the actual values were somewhat greater than forecast. Additionally, a mesoscale convective system (MCS)—one that did not appear in the analysis used for the model run—crossed South Dakota during the morning hours. The convection associated with the MCS altered the forecast instability fields somewhat.

The MCS in question began as an overnight squall line that stretched from North Dakota southward into western Nebraska. By 1100 UTC the segment moving through Nebraska had weakened, while the activity in the Dakotas had intensified and taken on characteristics more resembling a mesoscale convective complex (MCC; Maddox 1980). Figure 5a is a 10.7-μm GOES image of the mesoscale system at midmorning; Fig. 5b is an afternoon visible image centered over the same area. While the MCC (cold-top area in the upper center of the image) is seen to be quite active at 1650 UTC, later imagery shows that it had nearly completely dissipated by midafternoon (black arrows in Fig. 5b). However, even at this time, the system is still seen to be affecting the South Dakota–Nebraska area. Notice, in particular, the low-level thunderstorm outflow (LTO) boundary in southeastern South Dakota, represented by an arc of cumulus cloudiness stretching west-northwestward from the southeast tip of SD (white arrows). Such boundaries can play important roles in later thunderstorm development and evolution (e.g., Purdom 1976; Weaver 1979; Weaver et al. 1994; Davies et al. 1994; Weaver and Purdom 1995; Browning et al. 1997; Markowski et al. 1998). Note that this boundary stretches westward toward the deep convection that had just formed north of the South Dakota–Nebraska border.

Figure 6a provides further illustration of how the undiagnosed MCC modified the 6-h Eta Model forecast from the 1200 UTC run. The background image is the CIMSS version of the LI product from the *GOES-11* sounder. It is overlaid with the Eta Model, 6-h forecast

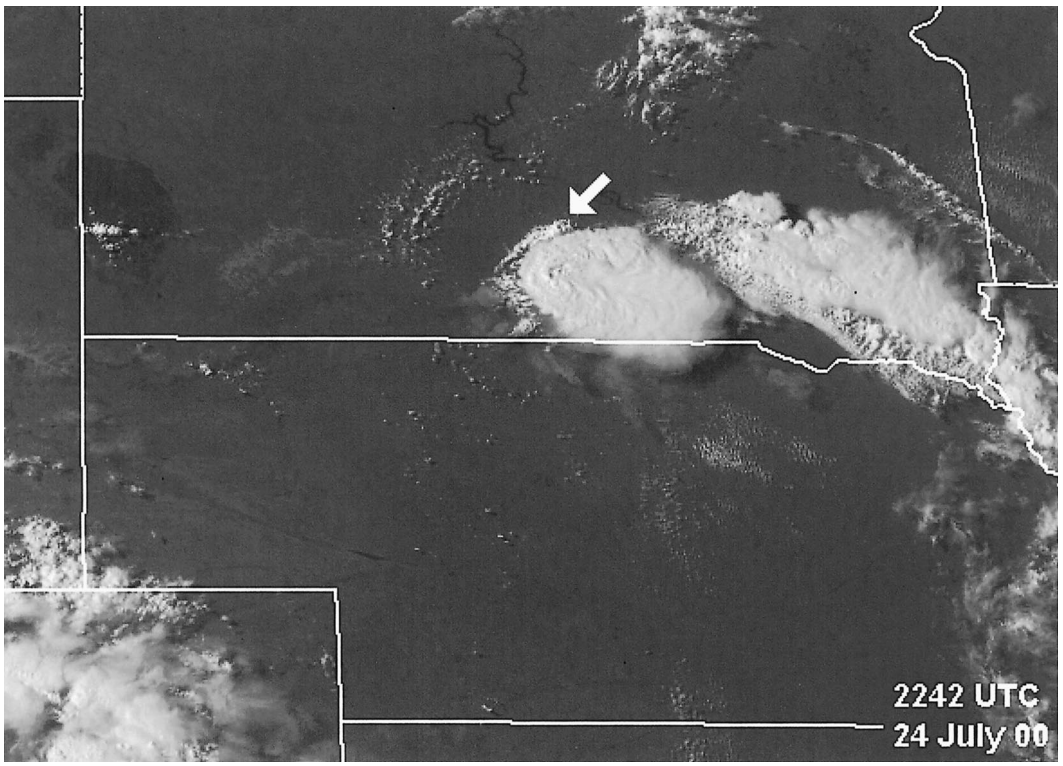

FIG. 9. *GOES-11* visible image taken at 2242 UTC 24 Jul 2000. Image shows the supercell thunderstorm in southern SD, with an LTO boundary along its northern and western edges. Arrow points to the left-moving thunderstorm that appeared after an apparent storm split.

LI fields. The model forecast finds the tongue of maximum instability (LI = −7) stretching from southwest Nebraska, northeastward into extreme northeastern South Dakota. Its orientation runs from about 210° to 30°. The real-time sounder data show a somewhat different picture. Eastern Nebraska is partly cloudy and is more stable than western sections of the state. This is reflected in the surface temperatures at midafternoon (Fig. 7). Also, the stable area north of the LTO boundary is still mostly cloud covered at this time and is reflected at the surface by a region of strong divergence (Fig. 7). Note that the divergence analysis finds the mesoscale LTO boundary to be situated somewhat farther south than the visible imagery shows it to be (cf. Figs. 5b and 7). However, the axis of convergence along the boundary separating cooler from warmer air in central Nebraska is located about where one would expect. The sounder product (Fig. 6) shows that the tongue of maximum instability is actually quite narrow and oriented from roughly 170° to about 350°, that is, nearly north–south. It intersects the LTO boundary in south-central South Dakota. Spotty, red pixels do show up just west of the MCS in Fig. 6a, but later imagery (cf. Fig. 6b) reveal that these values decrease through the early afternoon. On the plus side, it is interesting to note that the sounder-based values of LI are roughly the same magnitude (−7, −8) as those forecast by the Eta Model.

5. Mesoscale aspects of storm morphology

SRSO began at 1915 UTC, and at approximately 2130 UTC a thunderstorm formed near the intersection of the LTO boundary with the ridge of maximum, low-level instability. This ridge was collocated with the broad-scale convergence shown in Fig. 7. It should also be noted that the genesis region was just northeast of the surface low that was then located just southwest of Valentine, Nebraska (VTN in Fig. 7), and that the timing of the first storm formation coincided with the arrival of the shortwave trough from the west. It is not known whether any one of these factors played a singularly dominant role in storm formation, but certainly all four were potentially important factors.

Within 30 min of its formation, the storm appeared to develop right- and left-moving components. The main body continued to move south-southeastward, while a new core appeared on the north end of the original cell and began to separate. Data from the NWS Weather Surveillance Radar-1988 Doppler (WSR-88D) at Thedford, Nebraska, show this split clearly (Fig. 8). However, satellite imagery reveals that the process may not have

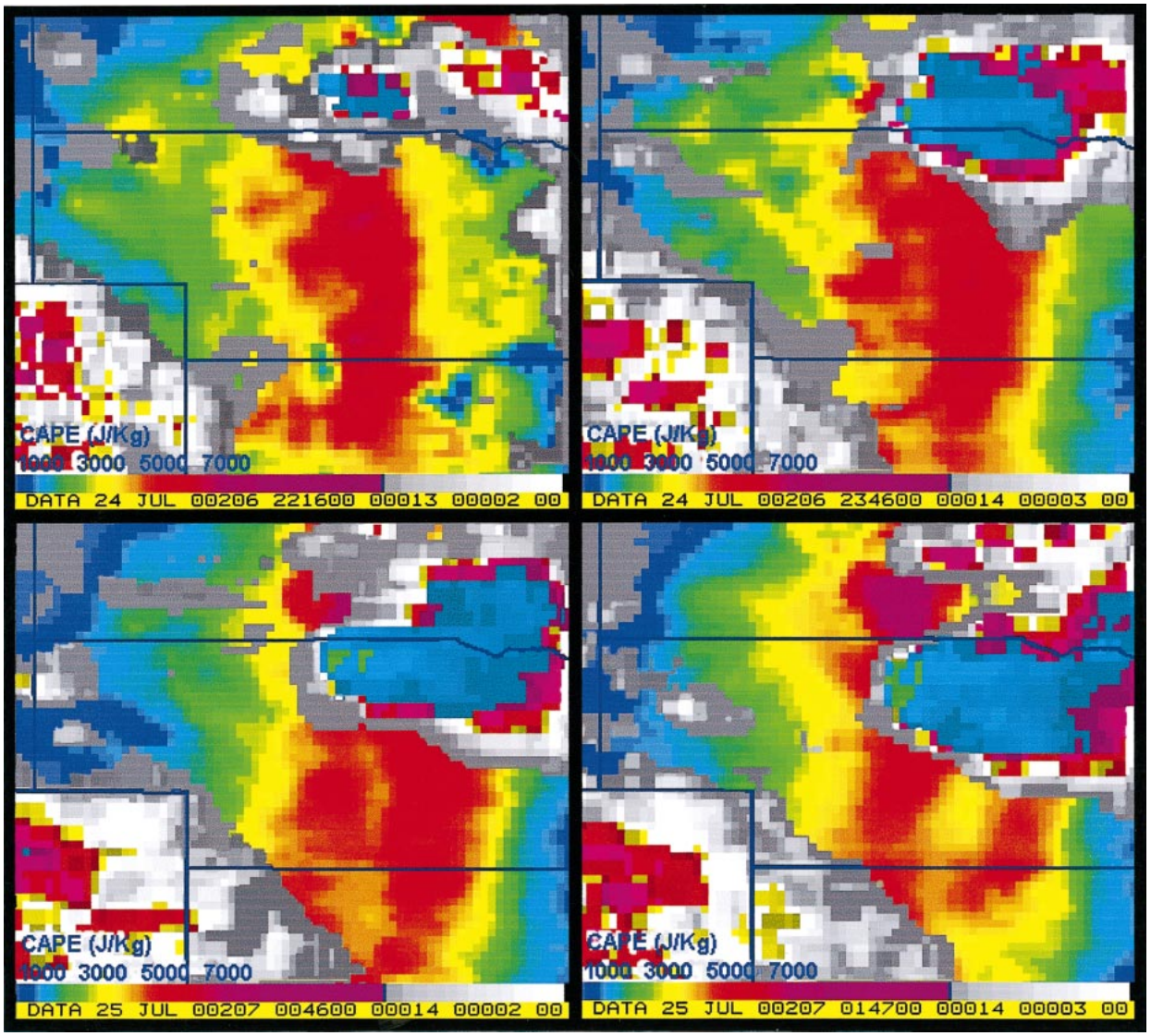

FIG. 10. SFOV, surface-based CAPE computed from *GOES-11* sounder data for various times: (top left) 2216 UTC 24 Jul 2000, (top right) 2346 UTC 24 Jul 2000, (bottom left) 0046 UTC 25 Jul 2000, and (bottom right) 0147 UTC 25 Jul 2000.

been a ''classical'' storm split, that is, one in which shear-induced pressure gradients on the flanks of the original updraft enhance lift, thereby producing two new updrafts (e.g., Rotunno and Klemp 1982, 1985). Figure 9, and especially sequential visible imagery,[3] show that the left-moving component in this case appears to have formed along a northward moving outflow boundary. Also, the imagery shows that when the new cell intersected the old LTO boundary that was associated with the MCS (discussed in section 4), it intensified discernibly and began moving east along the associated cloud line. Note that the hodograph was curved cyclonically in this case (Fig. 3). With this type of hodograph, in a classical storm-splitting situation, one should expect a region of high pressure to develop above the low pressure area on the left flank, causing the left-moving updraft to quickly dissipate (Wilhelmson and Klemp 1981). In this case, the left-mover did not dissipate, but continued east along the preexisting convergence line for more than 2 h and produced severe weather all along its path. It appeared to travel along the LTO boundary that had been created by the MCS earlier in the day in a manner similar to that discussed by Weaver (1979).

Sounder imagery products provide insight into the propagation mechanism of the right-mover. Figure 10

[3] Examples of animated visible and infrared satellite imagery from this case, along with WSR-88D loops, may be viewed online at [http://www.cira.colostate.edu/ramm/goes11/goes11_test/july24/july24.html.]

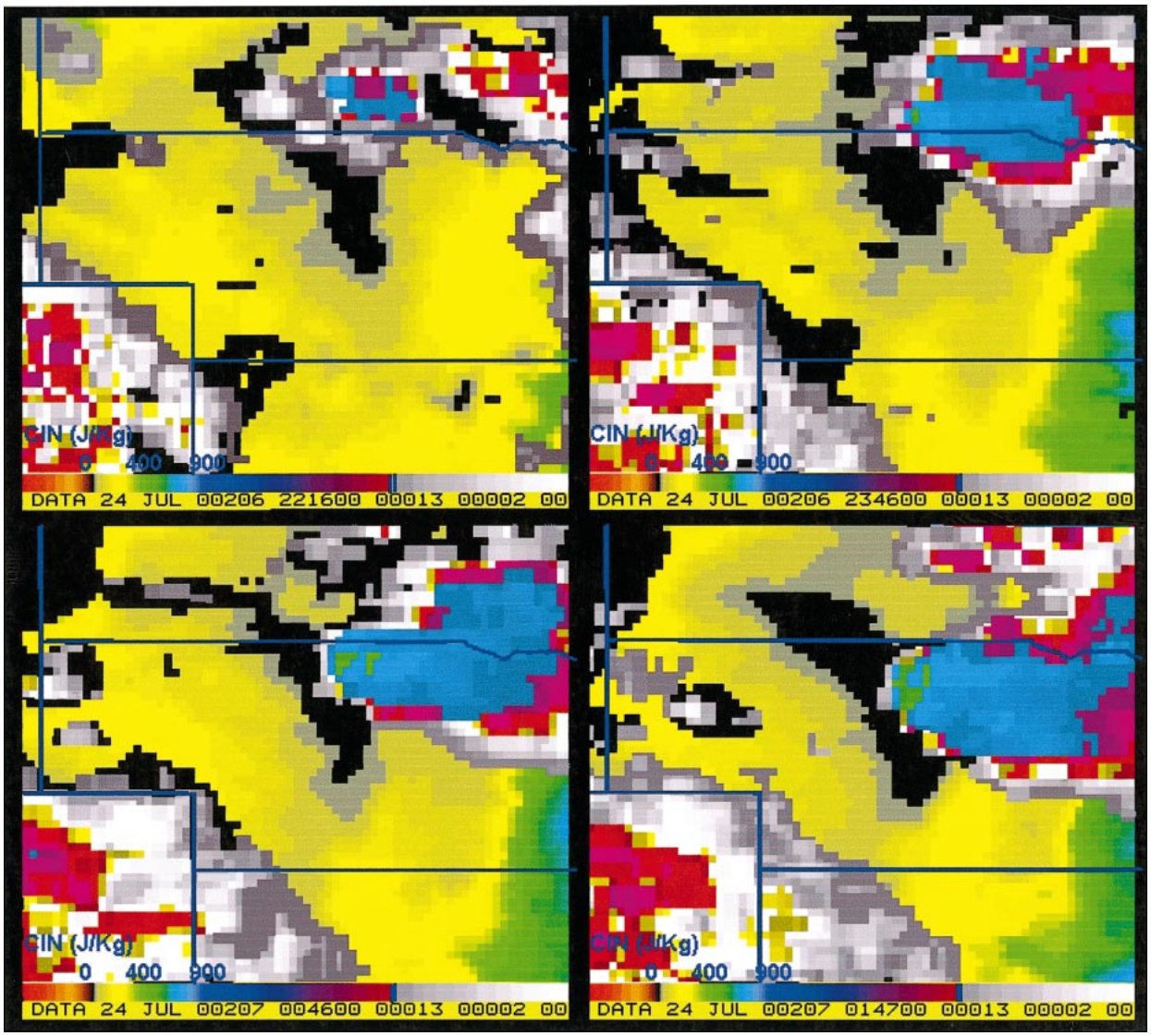

FIG. 11. SFOV, surface-based CIN computed from *GOES-11* sounder data for various times: (top left) 2216 UTC 24 Jul 2000, (top right) 2346 UTC 24 Jul 2000, (bottom left) 0046 UTC 25 Jul 2000, and (bottom right) 0147 UTC 25 Jul 2000.

shows examples of the NESDIS SFOV surface-based CAPE fields derived from *GOES-11* sounder data. Notice that the storm—which was moving from about 350°—seemed to have been propagating along the axis of highest CAPE, which, in turn, was situated along and near the north–south convergence boundary. Furthermore, the path of the most intense new development coincided with a narrow tongue of eroding CIN as computed from the same half-hourly sounder data (Fig. 11). It is possible that the storm was propagating south along this convergence boundary with new updrafts growing at the leading edge of its own outflow in a manner similar to that described by Weaver and Nelson (1982). Animated reflectivity data show new towers growing in a quasi-discrete fashion ahead of the most intense cores (e.g., Fig. 12).

We cannot know for certain whether the erosion of the low-level inversion resulted from low-level convergence, storm-scale dynamics, the approaching shortwave trough, or a combination of all three. However, the CIN sounder product may provide some insight as to the intensity of the shortwave. Had the shortwave trough been the dominate mechanism, one would expect the associated vertical velocity, and consequent layer lifting, to have been eroding the capping inversion in a broad region ahead of its approach. This did not occur to any noticeable degree. Since zero CIN values in Nebraska seem to be concentrated along the axis of low-

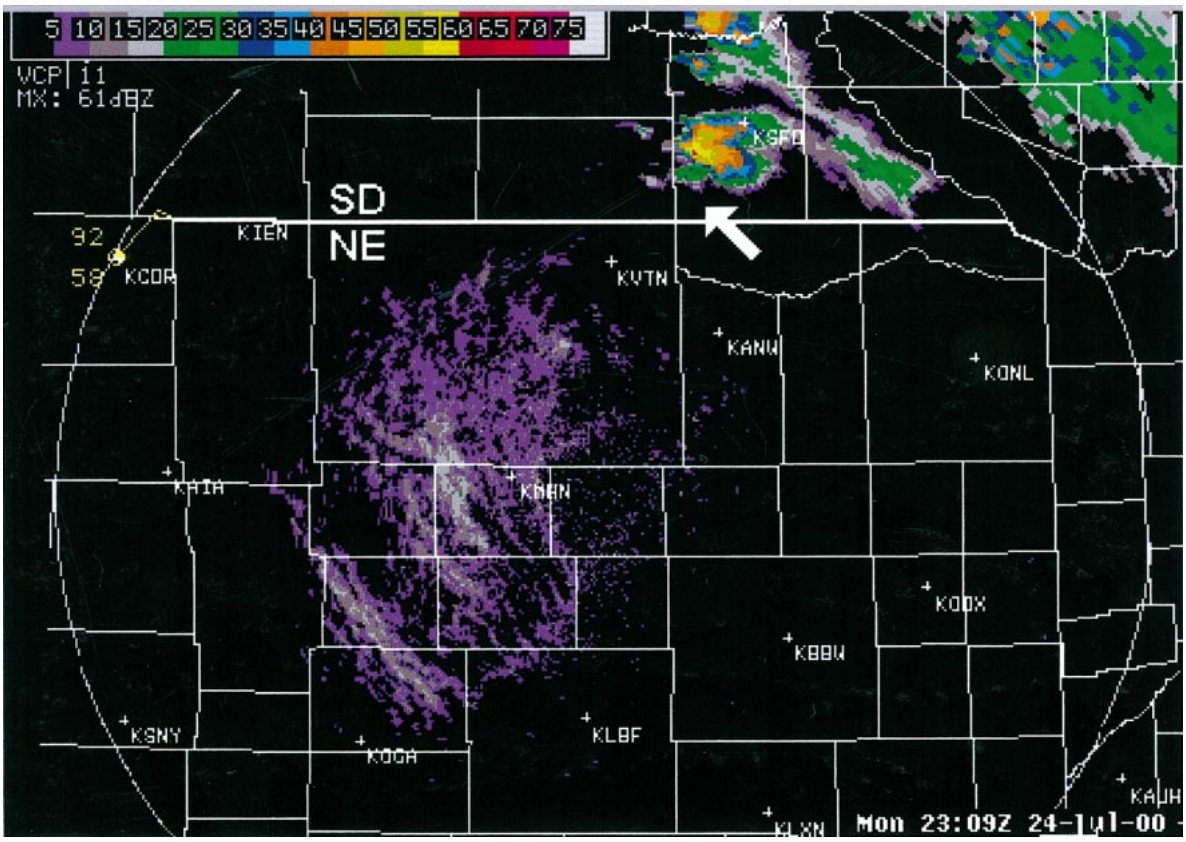

FIG. 12. The 0.5° tilt, PPI radar reflectivity data from the WSR-88D located at KLNX. Scan time is 2309 UTC 24 Jul 2000. Arrow points to new reflectivity core growing to the south of the main core as the supercell hybrid propagates south toward the NE border from SD.

level convergence, it is likely that this was the dominate forcing mechanism. Regardless of what specific mechanisms were involved in the erosion of the low-level capping inversion, the important point here is that the forecaster could watch the erosion taking place on the DPI–CIN. These data show that the right-mover's motion could readily be explained by factors other than shear-induced pressures, though the effects of the shear cannot be eliminated.

As an interesting sidebar to the main topic of this paper, we note without further comment a phenomenon that was first picked out on the continuous 1-min-interval imagery. Figure 13 shows two visible images leading up to the time the right-mover developed tornadic activity. The arrow in Fig. 12b points to a set of flanking towers that appeared suddenly on the west side of the storm about 10–15 min before the first tornadic activity and remained in place for as long as the tornadoes continued. These flanking towers formed above the outflow dome the storm was leaving behind itself. Similar occurrences have been seen in the past (e.g., Scofield and Purdom 1986; Weaver and Purdom 1995), but no explanation as to the reason for their sudden appearance, nor their relationship to tornadic activity, has been offered. It should also be mentioned that, though the feature was first noted on animated SRSO imagery, it could readily be picked out on an image loop constructed after the fact with visible images chosen at intervals that simulate standard rapid-scan operations (RSO) scheduling.

6. Concluding remarks

The *GOES-11* science test was completed successfully. All instrument performance characteristics were adjudged nominal. In mid-August, the satellite was placed in standby orbit, awaiting its time of service. This will happen when either *GOES-East* or *GOES-West* fails. As always, the opportunity to collect continuous rapid-scan data was illuminating and useful to the satellite research community. The case presented in this paper is one of several collected during the 3-week test period. Most of these cases clearly illustrate the relevance of both frequent-interval imager and sounder data in the forecast/nowcast cycle.

Both GOES sounder and imager data were found to provide valuable forecast information for nearly every aspect of the convective evolution on 24 July 2000. On the synoptic scale, GOES visible and 10.7-μm images furnished a tool for the quick identifications of an early morning MCS, and the GOES sounder data clearly showed the ramifications of this early activity on the

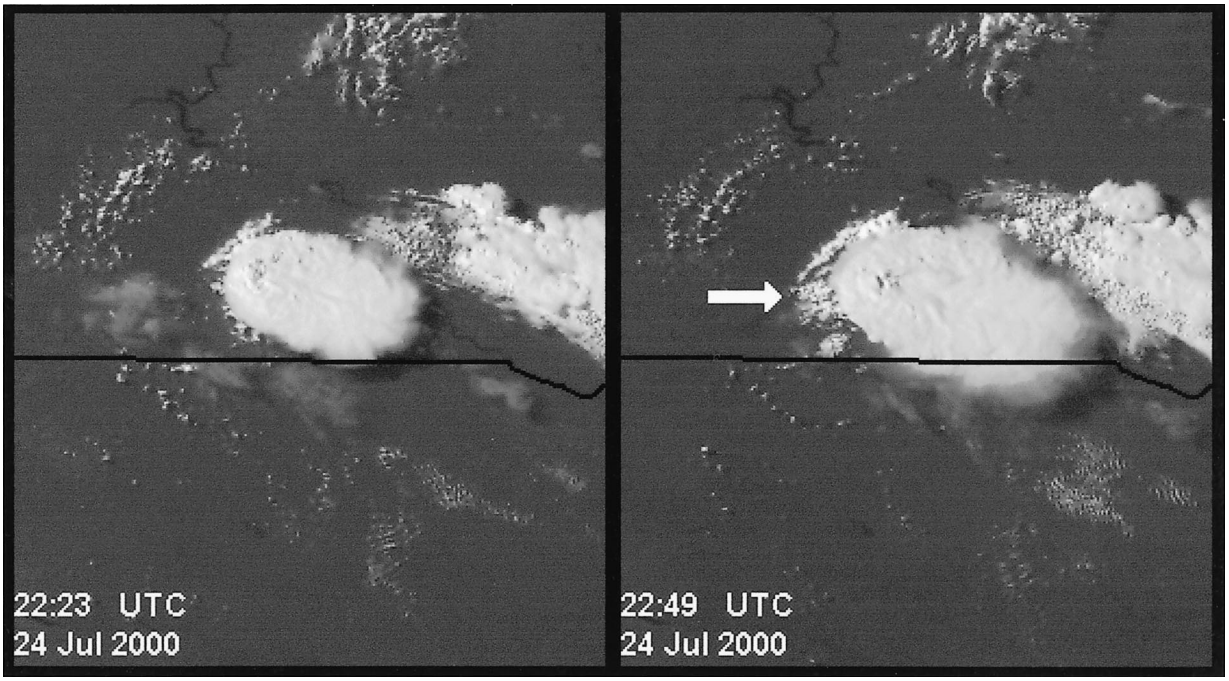

FIG. 13. Visible satellite images taken at 2223 and 2249 UTC, respectively, 24 Jul 2000. Arrow points to multiple flanks on the west side of the storm that developed over a 10–15-min period just in advance of tornadic activity.

late afternoon instability fields. By 1) combining these output with the knowledge of how thunderstorm outflows can alter in situ air masses and, later, 2) realizing the critical role that both low-level CAPE and CIN can play in the convective cycle, one can diagnose why the South Dakota–Nebraska storms formed where they formed, why they traveled in the direction they did, and why the southward-moving supercell lasted for as long as it did. Both 1- and 5-min-interval imagery allowed for continuous monitoring of the two principal storm components. The left-moving component was followed continuously on visible imagery. Animated imagery was especially helpful in establishing that the left-mover propagated along the LTO boundary associated with the MCS, which had occurred earlier in the day. This factor accounts for why the normally dissipative left-mover survived for more than 2 h as it produced large hail and damaging winds.

The 24 July 2000 case illustrates that both frequent-interval satellite data and sounder data can provide useful analysis tools for use in the warning decision making process. While many forecasters believe that sounder DPI have little relevance in the warning cycle—that sounder information may be more applicable to updating convective outlooks—this case has illustrated how such data can provide supplementary information about the environment in which storms are taking place. Information from satellites can have direct application in the warning cycle. In this case, the sounder products revealed a narrow, north–south tongue of instability stretching across Nebraska into northern Kansas. The right-mover seemed to be propagating southward along this feature as it produced its severe weather, though it is unknown how much of a role the high-CAPE–low-CIN combination played in controlling storm motion. Clearly, it played a role in the storm's longevity. The instability tongue did not weaken after sunset, providing clear justification for continuing to issue warnings for as long as the association between the two continued.

No convective activity formed ahead of the right-moving storm. The reason for the lack of activity was a ramification of the strong capping inversion (marked by moderate values of CIN) that dominated the area south of the storm throughout most of the forecast period. The DPI–CIN made it clear that the area well ahead of the southward moving supercell was strongly capped, that the encroaching shortwave trough was having little effect in removing this cap, and that, therefore, the region would most probably remain clear of convection. By identifying this limiting factor, the forecaster might then have been able to focus more attention on the active supercell alone—at least in the very short range forecast time frame. By understanding the evolving convective environment, the meteorologist involved in warning decision making can formulate a more accurate and precise short-range convective forecast, anticipate warning extensions or cancellations, and focus attention on areas favoring convective development and propagation.

While many forecasters seem to believe that satellite imagery and sounder data have little to offer in the short-fused world of warning decision making, and that the warning process should be governed strictly by radar

signatures and spotter information, this paper has shown that by concurrently monitoring imagery and/or sounder products, the forecaster may gain insight into the near-storm environment otherwise unavailable. This insight can put the storm(s) into a broader context and allow the analyst to understand and better predict important aspects of storm behavior.

Acknowledgments. A portion of the research presented in this study was performed under NOAA Grant NA67RJ0152. The authors would like to thank CIRA reviewers Dr. Mark DeMaria, Dr. Louis Grasso, and Mr. Jack Dostalek for their insightful comments on various drafts of this manuscript, as well as Dr. John R. Scala, whose formal critique and suggestions helped make the final version considerably stronger.

REFERENCES

Browning, P., J. F. Weaver, and B. Connell, 1997: The Moberly, Missouri, tornado of 4 July 1995. *Wea. Forecasting,* **12,** 915–927.

Davies, J. M., C. A. Doswell III, D. W. Burgess, and J. W. Weaver, 1994: Some noteworthy aspects of the Hesston, Kansas, tornado family of 13 March 1990. *Bull. Amer. Meteor. Soc.,* **75,** 1007–1017.

Hayden, C. M., G. S. Wade, and T. J. Schmit, 1996: Derived product imagery from *GOES-8. J. Appl. Meteor.,* **35,** 153–162.

Ma, X. L., T. J. Schmit, and W. L. Smith, 1999: A nonlinear physical retrieval algorithm—Its application to the *GOES-8/9* sounder. *J. Appl. Meteor.,* **38,** 501–513.

Maddox, R. A., 1980: Mesoscale convective complexes. *Bull. Amer. Meteor. Soc.,* **61,** 1374–1387.

Markowski, P. M., E. N. Rasmussen, and J. M. Straka, 1998: The occurrence of tornadoes in supercells interacting with boundaries during VORTEX-95. *Wea. Forecasting,* **13,** 852–859.

Menzel, W. P., and J. F. W. Purdom, 1994: Introducing GOES-I: The first of a new generation of geostationary operational environmental satellites. *Bull. Amer. Meteor. Soc.,* **75,** 757–781.

——, F. C. Holt, T. J. Schmit, R. M. Aune, A. J. Schreiner, G. S. Wade, and D. G. Gray, 1998: Application of *GOES-8/9* soundings to weather forecasting and nowcasting. *Bull. Amer. Meteor. Soc.,* **79,** 2059–2077.

Purdom, J. F. W., 1976: Some uses of high-resolution GOES imagery in the mesoscale forecasting of convection and its behavior. *Mon. Wea. Rev.,* **104,** 1474–1483.

Rotunno, R., and J. B. Klemp, 1982: The influence of the shear-induced pressure gradient on thunderstorm motion. *Mon. Wea. Rev.,* **110,** 136–151.

——, and ——, 1985: On the rotation and propagation of simulated supercell thunderstorms. *J. Atmos. Sci.,* **42,** 271–292.

Schmit, T., 1996: Sounder bias correction of the east-west radiance gradient. *Goes-8 and Beyond,* E. R. Washwell, Ed., *Proc. SPIE,* **2812,** 630–637.

Scofield, R. A., and J. F. W. Purdom, 1986: The use of satellite data for mesoscale analyses and forecast applications. *Mesoscale Meteorology and Forecasting,* P. S. Ray, Ed., Amer. Meteor. Soc., 118–150.

Weaver, J. F., 1979: Storm motion as related to boundary-layer convergence. *Mon. Wea. Rev.,* **107,** 612–619.

——, and S. P. Nelson, 1982: Multiscale aspects of thunderstorm gust fronts and their effects on subsequent storm development. *Mon. Wea. Rev.,* **110,** 707–718.

——, and J. F. W. Purdom, 1995: An interesting mesoscale storm–environment interaction observed just prior to changes in severe storm behavior. *Wea. Forecasting,* **10,** 449–453.

——, J. F. W. Purdom, and E. J. Szoke, 1994: Some mesoscale aspects of the 6 June 1990 Limon, Colorado, tornado case. *Wea. Forecasting,* **9,** 45–61.

Wilhelmson, R. B., and J. B. Klemp, 1981: A three-dimensional numerical simulation of splitting severe storms on 3 April 1964. *J. Atmos. Sci.,* **38,** 1581–1600.